Figure 8.1

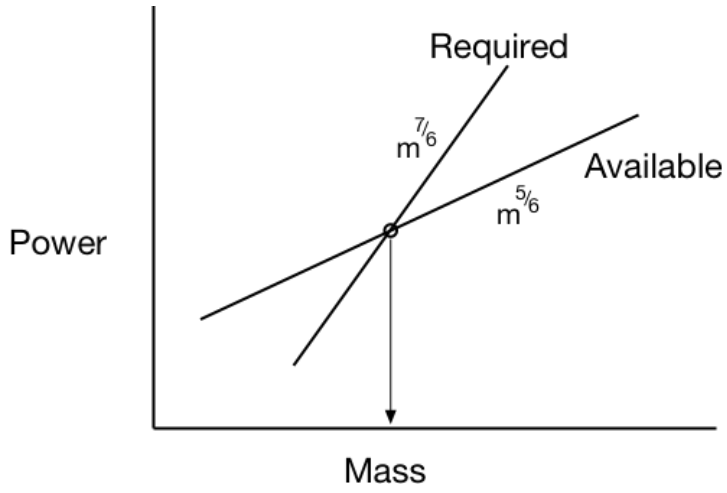

Conceptual relationship between required and available power for flying vertebrates, assuming standard isometric scaling.

Figure 8.2

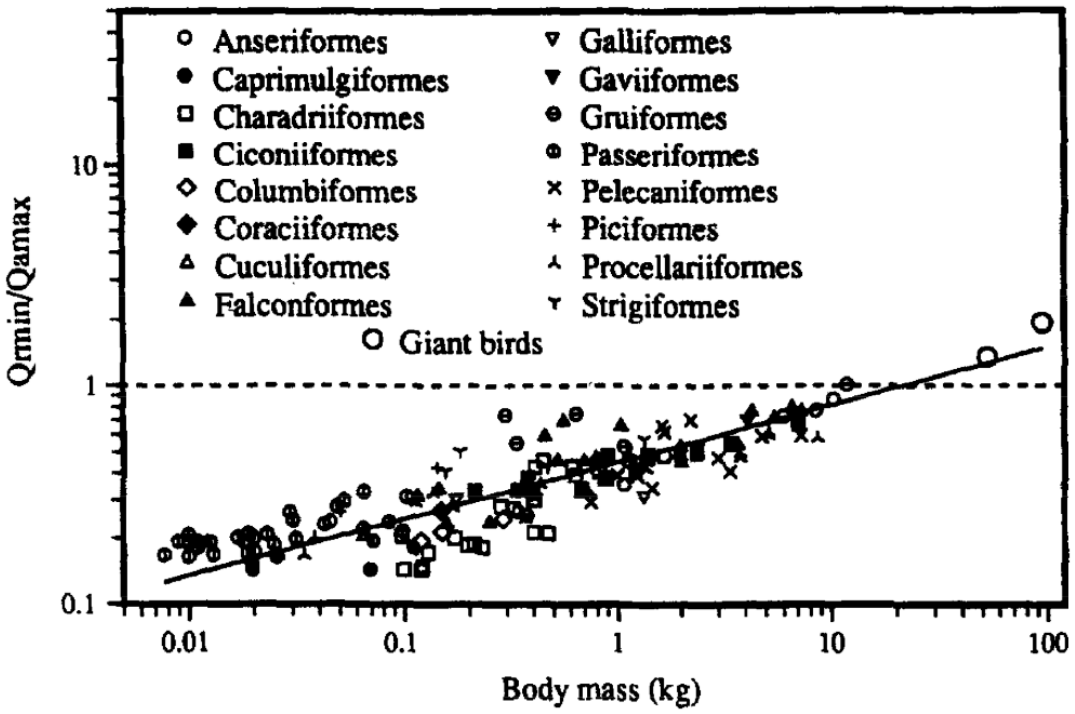

Graph (copied from Pennycuick 1996), showing a method of estimating the upper limit to the size of birds. The vertical axis is a measure of the ratio of available to required power: when the ratio = 1, the two are equal, which is taken as an indicator of the upper limit to size. The data represents a wide range of bird species and a standard major axis regression line is drawn through them. Extrapolation of this line suggests that the upper limit to the size of an “average bird” is around 15kg.

Figure 8.3

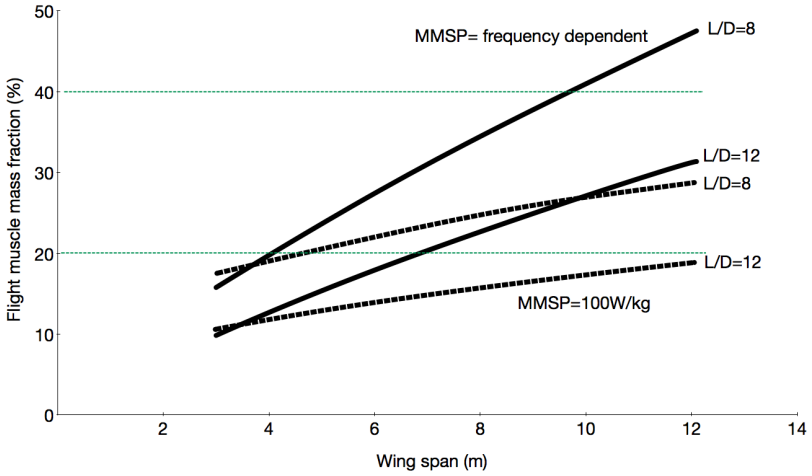

Variation of required flight muscle mass fraction with wing span, showing effect of variations in lift:drag ratio (L/D) and derivation of muscle mass specific power (MMSP). The solid lines are for a flapping frequency dependent muscle power (as proposed by Pennycuick 1996) and the broken lines for a constant value of 100W/kg (Ellington 1991). For the frequency dependent power the upper limit of 40% muscle mass fraction is breached at wingspan in the range from 10m to 15m depending on the L/D ratio, increasing to 15m or more for the constant power output assumption.

Figure 8.4

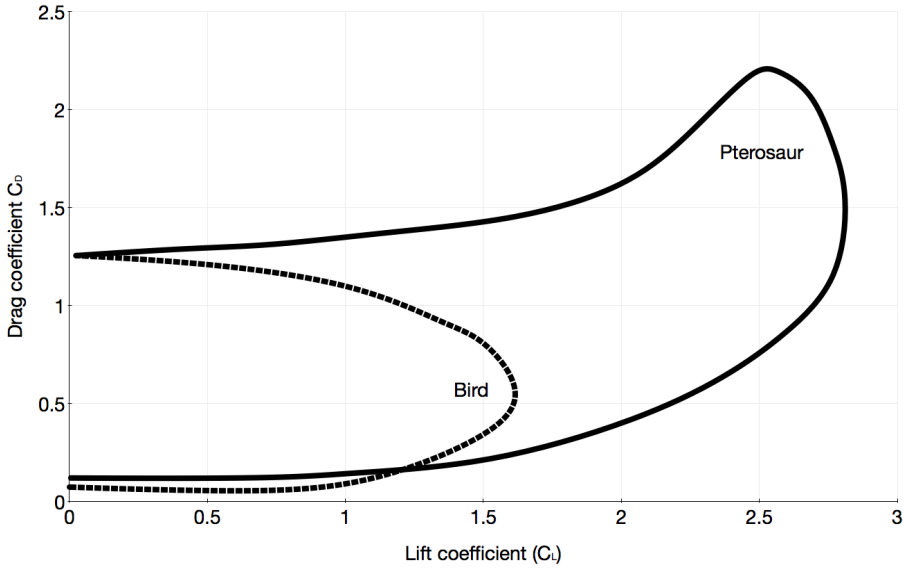

Aerodynamic polar curves of lift and drag coefficient for typical bird and pterosaur wing sections. The much higher maximum lift coefficient generated by the highly cambered pterosaur wing sections is immediately apparent.

Figure 8.5

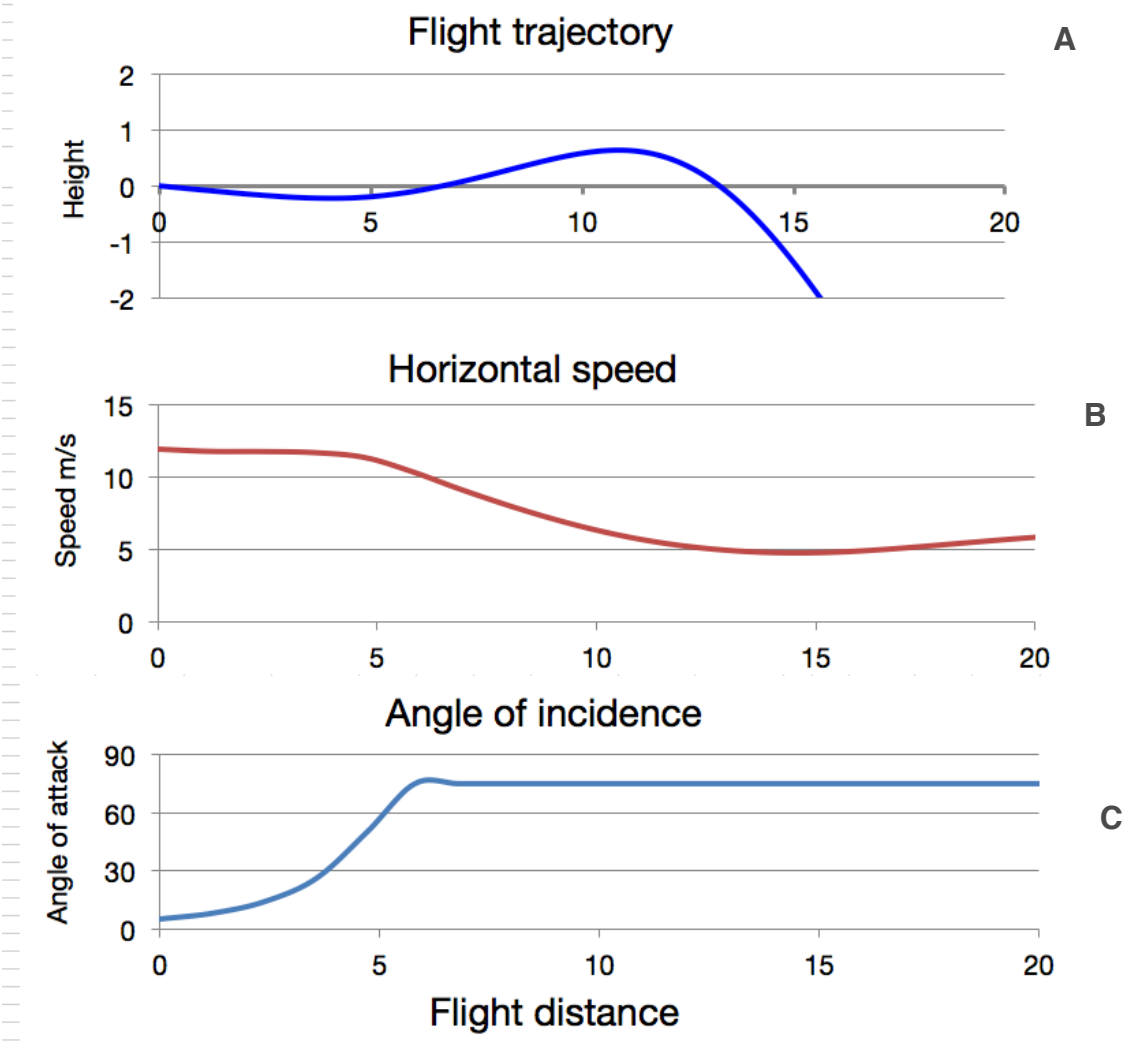

Screen grab of typical output of the landing dynamics time stepping calculation, showing (A) the flight trajectory, (B) the horizontal speed and (C) the angle of incidence of the wings, all plotted against a scale of distance in metres. The process of a rapid “pitch up” resulting in stall, which combines high lift and high drag, reduces the horizontal speed and after causing an initial gentle climb, produces a rapid descent in the final landing phase at around 15metres. In all cases the “pitch up” height was constrained to less than 1m.

Figure 8.6

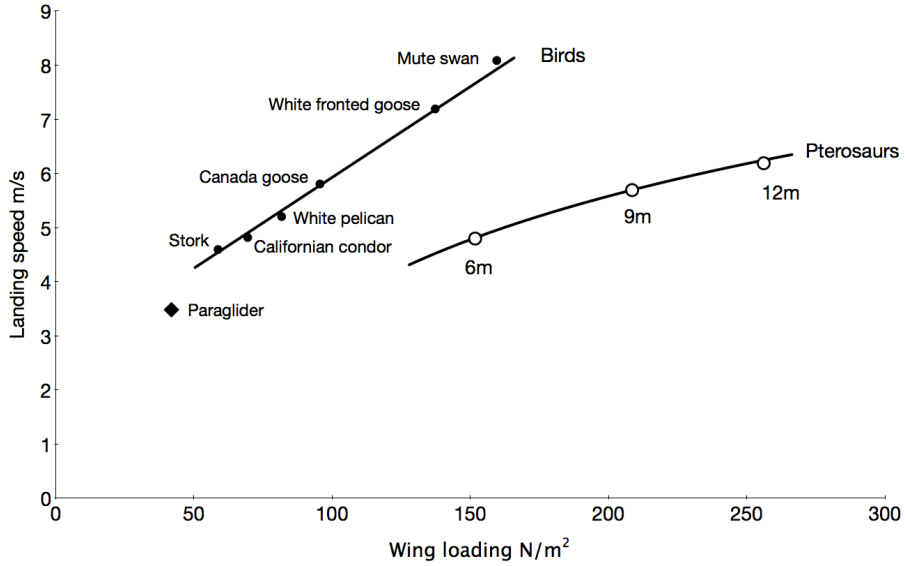

Calculated variation of landing speed with wing loading for birds and pterosaurs (with a human carrying paraglider included for comparison). Large, highly loaded birds such as swans have landing speeds approaching 8m/s, but this is reduced to 5m/s for equally sized, but lower wing loading species (e.g. Condor). Even the largest pterosaurs have landing speeds that are lower than for the fastest landing birds.

Figure 8.7

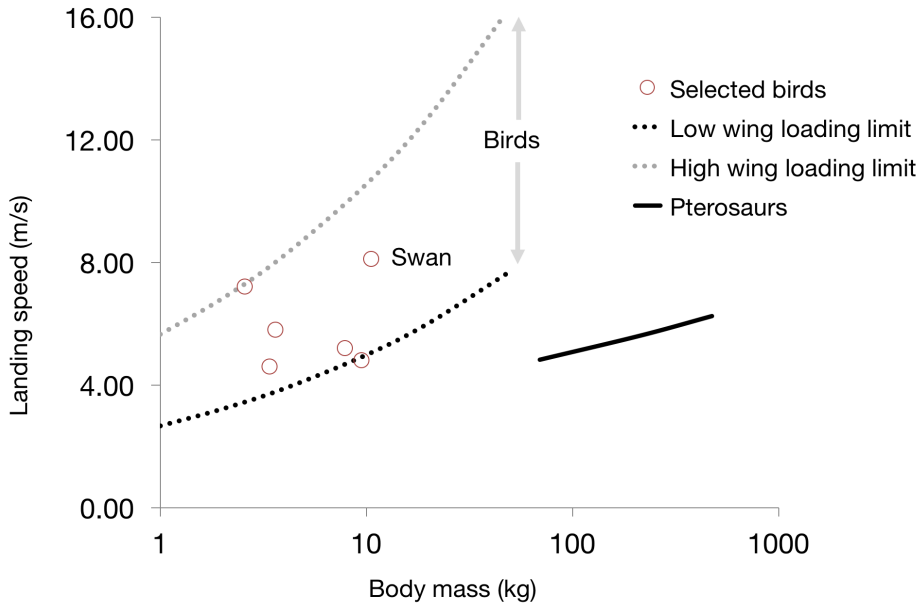

Data in Figure 8.6 recast in terms of body mass, again showing again the relatively much lower landing speeds calculated for pterosaurs.

Figure 8.8

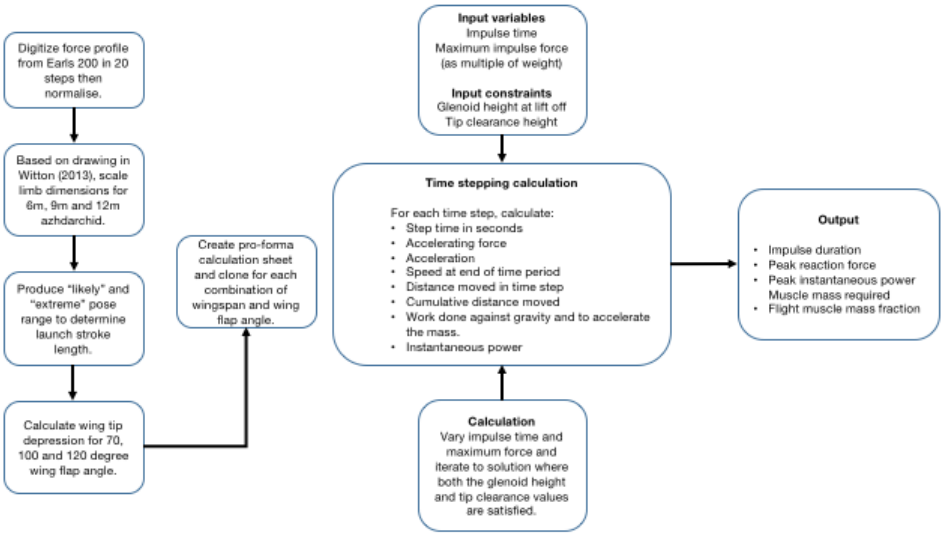

Descriptive flow diagram of the stages in the time stepping computer model of pterosaur launch. From left to right, first the defining assumptions are listed and then the actual calculation process inputs and outputs are defined.

Figure 8.9

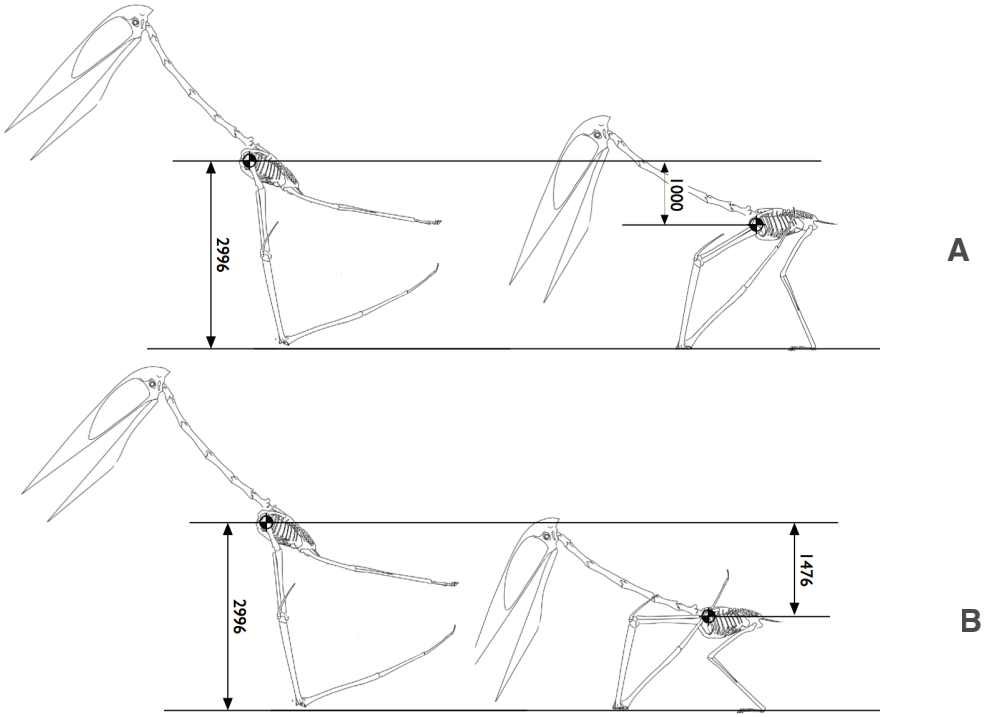

Illustrations used to determine the possible range of launch stroke angles. A: launching from a standing pose and B from an extreme crouched pose. Images generated from Witton (2013).

Figure 8.10

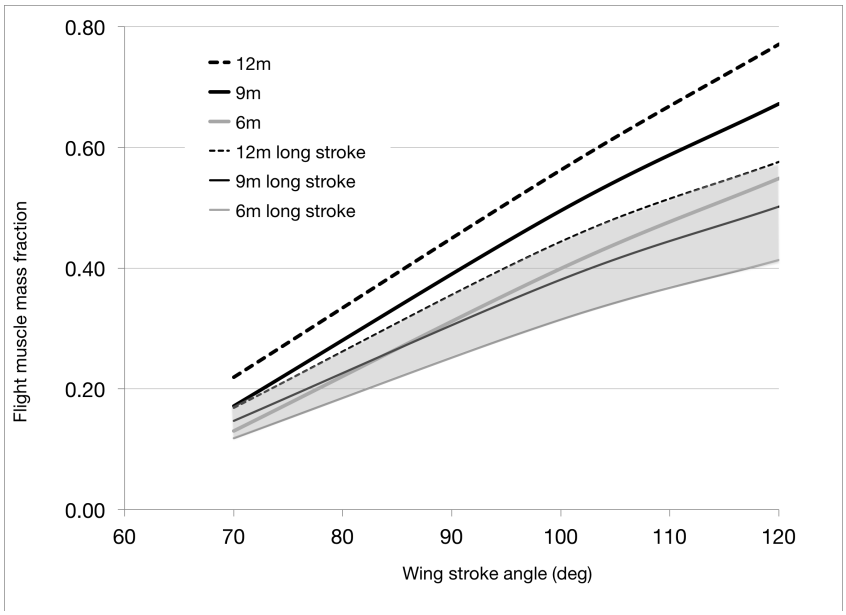

Relationships between required muscle mass fraction, animal size, launch stroke length and wing stroke angle. The shaded area groups the results for the long launch stroke, which for any particular wing stroke angle requires less power and hence muscle mass. A flight muscle mass fraction in excess of 40% is considered unlikely in pterosaurs, so for most of the simulated conditions, the wings stroke angle cannot exceed 100 degrees, which is somewhat lower than is the case in large birds.

Figure 8.11

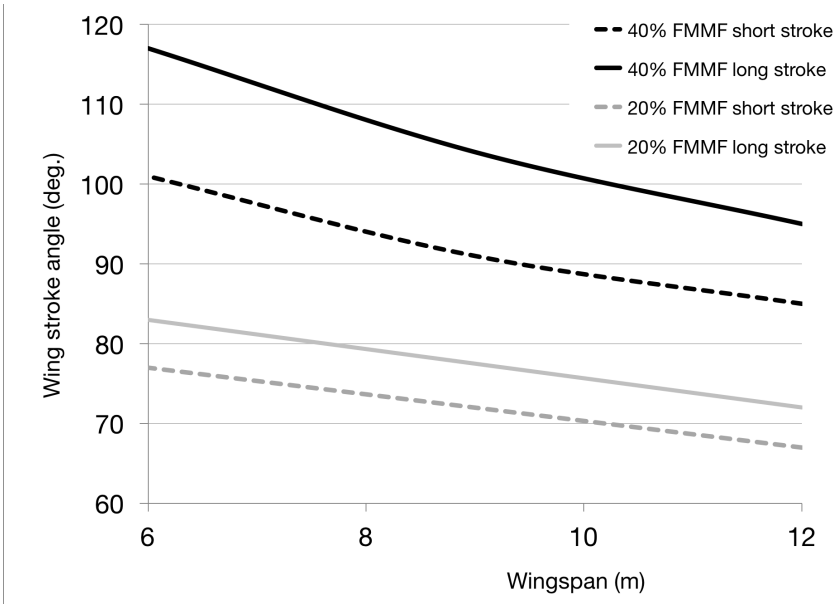

Results from Figure 8.10 replotted to show more clearly the variation with wing span. The upper, dark curves are for 40% FMMF and the lower lines for 20%, bracketing the likely range in pterosaurs. To achieve a wing stroke angle in excess of 90 degrees, the 12m size requires both a high FMMF and the ability to use the extreme launch stroke.

Figure 8.12

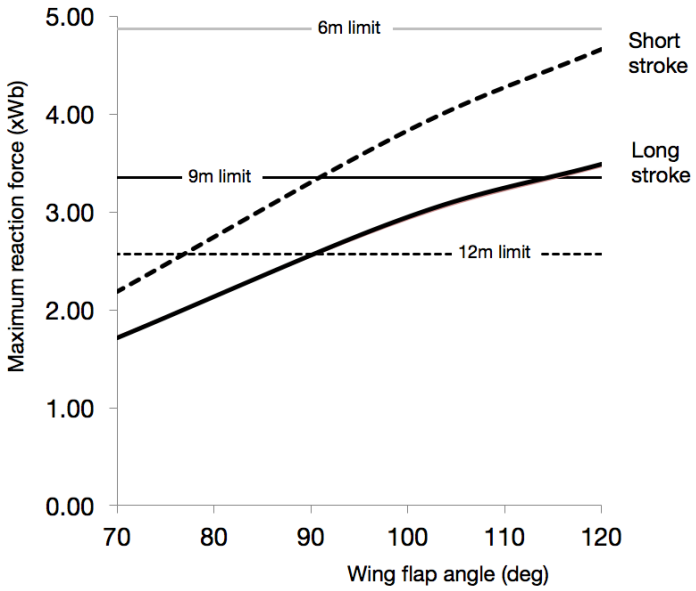

Peak launch ground reaction forces for different stroke lengths, with limits from Alexander (1985a) overlaid. Horizontal lines are the Alexander limits for the three different sized animals. Since the power scale is the ratio of force to weight, the results collapse on to the same lines for the three different sizes.